communications earth & environment

Article

A Nature Portfolio journal

https://doi.org/10.1038/s43247-025-02634-1

Unstable geogenic arsenic in reclaimed coastal soils poses environmental risks

Meng Chen[1,3], Yan Li[1,3], Yuting Zhang[2], Wenbing Ji[1], Yuanyuan Lu[1], Zhen Song[1], Lei Wang[1] ✉ & Tao Long[1] ✉

Rapid urbanization has driven extensive coastal land reclamation worldwide. However, the soils used often contain geogenic contaminants, particularly arsenic, posing a largely unrecognized but substantial threat to the environment and human health. Here we present a comparative analysis of arsenic speciation in naturally contaminated coastal soils, revealing distinct risk profiles between reclaimed and natural environments. Analysis of 1029 soil samples from the Pearl River Delta, with detailed characterization of 29 high-arsenic samples using integrated chemical and microscale techniques, identifies two contrasting arsenic occurrence patterns: reclaimed soils dominated by unstable arsenic sulfide species versus natural hilly soils characterized by stable arsenic oxide species. The findings demonstrate that land development activities, hydrological dynamics and sea-level rise can trigger arsenic release in reclaimed soils. To mitigate these risks, an integrated risk management framework is proposed. This research provides valuable insights to inform sustainable land reclamation management across rapidly urbanizing coastal regions.

Rapid coastal urbanization worldwide presents both opportunities and environmental challenges. Countries including China, Japan and Singapore have undertaken extensive land reclamation projects, with China reclaiming 13,380 km^2 between 1949 and 2016[1–4]. These activities disrupt the geochemical equilibrium of naturally occurring elements, particularly heavy metals and metalloids. Land reclamation alters key environmental parameters including pH, redox potential, soil water content, oxygen availability and mineral phase stability[5,6]. Among these elements, arsenic poses unique risks due to its high toxicity, complex redox chemistry and exceptional sensitivity to environmental changes[7,8].

The Pearl River Delta (PRD) exemplifies this challenge. Located within the South China fold system, the region's Mesozoic formations underwent tectonic and hydrothermal alterations that enriched arsenic in sulfide minerals[9]. Studies show elevated arsenic in reclaimed lands frequently exceeding regulatory standards[8,10]. Although no clinical arsenic poisoning cases have been reported from reclaimed areas in the PRD, naturally contaminated soils attract widespread concern due to potential health risks when disturbed by development activities[7,8].

Arsenic differs fundamentally from other heavy metals in its environmental behavior. While metals like Pb and Cd exist as cations, arsenic occurs predominantly as oxyanions (arsenate and arsenite) with pH-dependent mobility and complex redox transformations[11,12]. Arsenic speciation, rather than total concentration, governs its risks and behavior. It exists in various forms from primary sulfides to secondary phases associated with iron oxides and silicates[13,14]. Characterizing these diverse species requires integrated analytical approaches. Land reclamation can destabilize these phases through sulfide oxidation in aerobic conditions or reductive dissolution of iron oxides under reducing conditions[15–17].

Sequential extraction methods like BCR (Community Bureau of Reference) extraction provide operationally defined fractionation of heavy metals and metalloids including arsenic[18–21]. While these methods have operational limitations, they remain valuable for arsenic mobility assessment[20,22]. Advanced techniques offer complementary capabilities: Tescan integrated mineral analyzer (TIMA) for rapid mineral identification[23], electron probe microanalysis (EPMA) and plasma mass spectrometer (LA-ICP-MS) for trace arsenic characterization at ppm levels[24]. Integrating these techniques overcomes individual limitations, enabling comprehensive arsenic characterization across scales.

Recent studies have advanced our understanding of geogenic arsenic in various settings. Volcanic weathering and sulfide deposits have been highlighted as important factors in arsenic release[25], while relationships between arsenic speciation and sulfide minerals in contaminated soils have been revealed[7]. Arsenic speciation variations across mine sites have been demonstrated[26]. In the PRD, arsenic-rich soils (21–148 mg kg^{-1}) have been documented in reclaimed areas from Jurassic fill materials, exemplifying

[1]Nanjing Institute of Environmental Sciences, Ministry of Ecology and Environment of the People's Republic of China, Nanjing, China. [2]Guangdong Key Laboratory of Contaminated Environmental Management and Remediation, Guangdong Provincial Academy of Environmental Science, Guangzhou, China. [3]These authors contributed equally: Meng Chen, Yan Li. ✉e-mail: leiwang@nies.org; longtao@nies.org

how urban development relocates naturally enriched materials to surface environments[8].

However, comprehensive characterization of arsenic speciation in coastal reclaimed soils versus natural environments remains limited. Reclaimed areas possess unique characteristics: materials sourced from arsenic-enriched formations, altered redox conditions from land disturbance and vulnerability to sea-level rise[27–29]. These factors can trigger arsenic mobilization through sulfide oxidation and iron oxide dissolution, processes further influenced by pH changes and microbial activity. Understanding chemical speciation and mineralogical characteristics of arsenic in soils is crucial for risk assessment and land-use planning in coastal urban areas.

This study investigates geogenic arsenic in reclaimed and hilly soils of China's PRD using an integrated multi-scale approach combining BCR extraction, TIMA, EPMA, and LA-ICP-MS. Through comparative analysis, we characterize distinct arsenic speciation patterns and mineralogical assemblages across contrasting coastal environments, evaluate how land reclamation influences arsenic mobility, and assess associated environmental risks. Our findings provide essential insights for managing naturally contaminated soils in rapidly urbanizing coastal regions worldwide.

Results

Soil characteristics and arsenic content across geomorphological units

Soil physicochemical properties varied across three geomorphological units in the coastal urban environment ($n = 1029$, Fig. 1b–d and Supplementary Table S1). Reclaimed soils ($n = 775$) exhibited weak alkalinity (mean pH 7.64, 95% CI: 7.55–7.73) and relatively high arsenic content (mean 55.87 mg kg^{-1}, median 13.20 mg kg^{-1}), substantially exceeding China's regulatory screening threshold of 20 mg kg^{-1} (GB36600-2018). Most strikingly, these soils showed extreme spatial heterogeneity, with arsenic concentrations ranging from 0.23 to 553 mg kg^{-1} even between adjacent sampling points, contrasting sharply with the pronounced right-skewed distribution (median 13.20 mg kg^{-1}).

Hilly soils ($n = 81$) displayed marked acidity (mean pH 4.9, 95% CI: 4.73–5.07) with intermediate arsenic levels (mean 21.2 mg kg^{-1}, median 8.09 mg kg^{-1}) slightly exceeding the regulatory threshold. Alluvial soils ($n = 173$) were near neutral (mean pH 7.04, 95% CI: 6.82–7.26) with the lowest arsenic concentrations (mean 10.28 mg kg^{-1}, median 7.56 mg kg^{-1}), remaining below regulatory standards.

These distinct patterns reflect different formation processes and arsenic sources. The extreme heterogeneity and elevated arsenic in reclaimed soils result from randomly distributed fill materials sourced from arsenic-bearing geological formations (Supplementary Fig. S1). In contrast, hilly soils represent in-situ weathering products where acidic conditions influence arsenic retention through enhanced sorption to iron oxides at low pH[30], while prolonged leaching has partially depleted mobile arsenic fractions[31]. Alluvial soils, formed through sediment deposition, show the most homogeneous and lowest arsenic levels, reflecting dilution during transport and sorting processes[11].

Arsenic distribution and correlations in high-As soils

Comprehensive analysis of 29 high-arsenic soil samples (As > 20 mg kg^{-1}) revealed a large difference between reclaimed land and hilly slopes (Supplementary Table S2). Reclaimed soils ($n = 14$) showed higher and more variable As (range: 26.33–515.85 mg kg^{-1}; mean: 91.99 mg kg^{-1}) and S (range: 2142–32930 mg kg^{-1}; mean: 7578 mg kg^{-1}) contents, with two samples (CG007-1 and CG009-1) exhibiting exceptionally high values (515.85 and 213.21 mg kg^{-1}, respectively). Hilly soils ($n = 15$) displayed comparatively lower As (range: 24.83–129.49 mg kg^{-1}; mean: 66.95 mg kg^{-1}) and S (range: 487–1973 mg kg^{-1}; mean: 989 mg kg^{-1}) contents. These findings highlight the distinct As occurrence characteristics in different geomorphological units.

Correlation analysis revealed complex relationships between arsenic and other elements across different geomorphological units. Pearson's correlation analysis was performed to examine potential mineralogical controls on arsenic distribution. As shown in Fig. 1e, a weak positive correlation between As and Fe contents ($r = 0.30$, $p = 0.27$, $n = 29$) suggests a potential, though statistically non-significant, association of As with Fe-bearing minerals. Notably, in reclaimed soils, we also find a positive correlation between Fe and S contents ($r = 0.80$, $p < 0.001$, $n = 14$), indicating more complex arsenic-bearing mineral compositions potentially controlled by both primary sulfides and secondary Fe oxides[7,8]. In contrast, hilly soils exhibited a moderate correlation between Fe and S ($r = 0.49$, $p = 0.06$, $n = 15$), suggesting a different mineral assemblage and weathering history[31,32].

Hilly soils exhibited an increasing trend of arsenic content with depth, possibly reflecting the combined influence of weathering processes and parent material on arsenic enrichment. These observations align with recent studies on metal concentration trends in soil profiles of arsenic-rich areas[26]. However, arsenic distribution in soil profiles has been shown to be highly heterogeneous, with high concentrations potentially occurring at various depths[33].

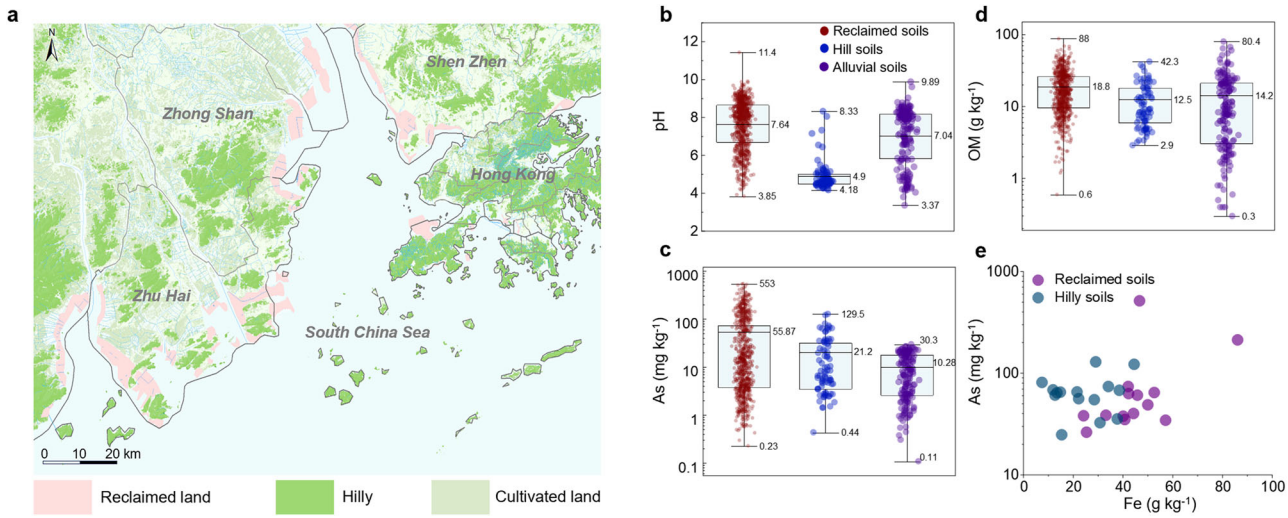

Fig. 1 | Study area and soil properties across three geomorphological units. **a** Distribution of reclaimed land, hilly and cultivated land in the study area. **b** pH. **c** Arsenic. **d** Organic matter. **e** Relationship between As and Fe contents in 29 reclaimed and hilly soils. Data from 1029 soil samples from reclaimed lands ($n = 775$), hilly slopes ($n = 81$) and alluvial plain ($n = 173$). Scatter plots show individual samples (red circles represent reclaimed soil, blue circles represent hill soil, purple circles represent alluvial soil); box plots display five-number summary statistics (maximum, minimum, 25th and 75th percentiles and mean values).

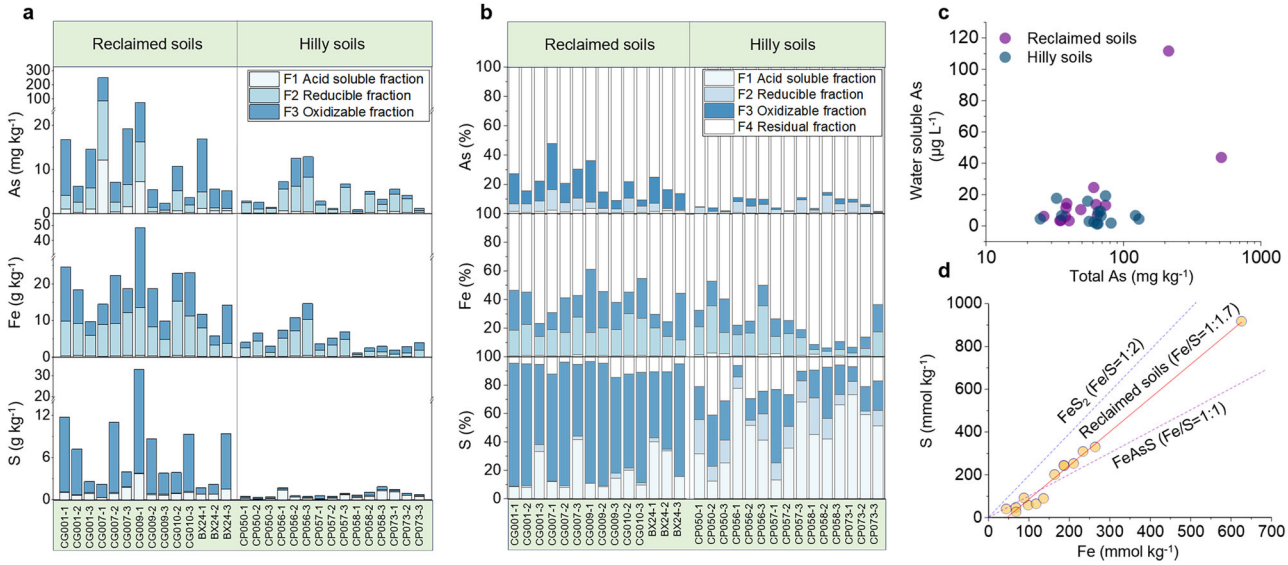

Fig. 2 | BCR fractionation and element relationships in 29 high-arsenic soil samples from reclaimed lands and hilly slopes. a Content distribution of As, Fe and S fractions. **b** Percentage distribution of As, Fe and S fractions. **c** Total As vs. water-soluble As content. **d** Relationship between oxidizable Fe and S in 14 reclaimed soils.

As, Fe and S fractionation in reclaimed and hilly soils

Results from total element analysis and correlation studies indicate that arsenic occurrence and enrichment mechanisms are associated with multiple mineral phases, particularly iron-bearing minerals and sulfides. BCR analysis further revealed marked differences in As, Fe, and S speciation distribution between reclaimed and hilly soils (Fig. 2a, b), reflecting distinct geochemical characteristics and soil formation processes. This difference primarily stems from the unique origin of reclaimed soils, derived from surrounding geological formations that naturally contain elevated levels of arsenic and other trace elements. These source materials contribute to the complex speciation patterns observed in reclaimed lands, highlighting the need for in-depth investigation of arsenic behavior in these complex soil systems.

Residual As (F4) predominated in both geomorphological units (Supplementary Table S3), with higher proportions in hilly soils (mean 93.07%) compared to reclaimed soils (mean 77.87%). Reclaimed areas showed substantially higher oxidizable As (F3) content (mean 21.30 mg kg^{-1}, 14.96%) than hilly terrains (mean 1.43 mg kg^{-1}, 1.89%), with samples CG007-1 and CG009-1 exhibiting exceptionally high values (165.73 mg kg^{-1} and 57.19 mg kg^{-1}, respectively). Reclaimed soils also contained higher levels of reducible (F2) and weak acid-extractable (F1) As, indicating greater arsenic mobility and potential bioavailability. Notably, only a weak correlation was observed between total As content and water-soluble As ($r = 0.54$), which disappeared ($r = -0.05$) after removing two extreme values (Fig. 2c). This finding, consistent with Itabashi[7], emphasizes that soil As solubility is not directly related to its total concentration, highlighting the importance of speciation studies in assessing arsenic mobility and bioavailability in these complex soil systems.

Fe and S speciation analysis further indicate the distinct geochemical characteristics of reclaimed and hilly soils. Despite similar total Fe contents, reclaimed soils showed higher reducible (F2) and oxidizable (F3) Fe fractions, with sample CG009-1 exhibiting an exceptionally high oxidizable Fe content (34.94 g kg^{-1}). Sulfur speciation also differed markedly, with reclaimed areas showing higher proportions (mean 71.70%) and absolute content (mean 6.7 g kg^{-1}) of oxidizable S (F3) compared to hilly terrains (mean 191 mg kg^{-1}, 22.10%). As shown in Fig. 2d, a linear relationship between oxidizable Fe and S in reclaimed samples, with a slope (1.7) lower than the theoretical FeS_2 molar ratio, suggested the presence of various Fe sulfides, including arsenopyrite (FeAsS) or arsenic-bearing pyrite ($Fe(As,S)_2$). These findings indicate that Fe minerals likely serve as important As carriers in reclaimed soils, with complex sulfide compositions influencing As behavior.

These findings highlight differences in As, Fe and S speciation between reclaimed and hilly soils. Reclamation soils exhibited higher element mobility and potential bioavailability, particularly in oxidizable forms, indicating an important role of various sulfides in As retention. Reclaimed areas contain unweathered materials with preserved primary arsenic sulfides, while hilly soils underwent millennia of weathering, transforming minerals into stable secondary phases. Reclamation alters the original redox environment, potentially leading to arsenic release from previously stable primary minerals, particularly sulfides. In contrast, elements in hilly soils predominantly exist in residual forms, indicating higher geochemical stability. To comprehensively understand arsenic occurrence and potential environmental risks, we complemented the BCR extraction with advanced mineralogical analysis techniques, including TIMA and EPMA.

Microscale characterization of arsenic-bearing species

To further elucidate the mineralogical controls on arsenic behavior, we employed TIMA technology for comprehensive, high-resolution analysis of soil samples. Each sample analysis covered 0.9–2.5 million particles (489 mm^2 circular target), with cumulative X-ray acquisition points reaching 6.89–26.74 million. Microanalytical data reliability was ensured through EPMA ZAF matrix correction with extended As counting times and LA-ICP-MS calibration using NIST standards with regular verification. Figure 3 demonstrates the high resolution of TIMA in identifying submicron particles, comparing phase distribution maps with backscattered electrons (BSE) images, mineral phase distributions and As element mapping of selected regions (M1-M4) for sample CG007-1. TIMA analysis revealed quartz as the predominant mineral phase (49.39–81.59%) in all samples, followed by various silicates, reflecting parent material characteristics and weathering processes. Differences in As-bearing phases (As-S and As-O species) were observed between reclaimed areas and hilly terrains, indicating distinct soil-forming environments and the impact of anthropogenic activities on soil geochemical properties (Supplementary Table S4).

Reclaimed soils showed higher contents of pyrite (up to 6.64% in CG009-1) and Fe (hydr)oxides (2.66-3.97%) compared to hilly soils. Secondary phases like jarosite and natrojarosite, indicators of sulfide oxidation and arsenic carriers in oxidizing environments, were identified in reclamation samples[31]. This mineralogical distinction likely results from unique reclamation materials and post-reclamation conditions, with reducing

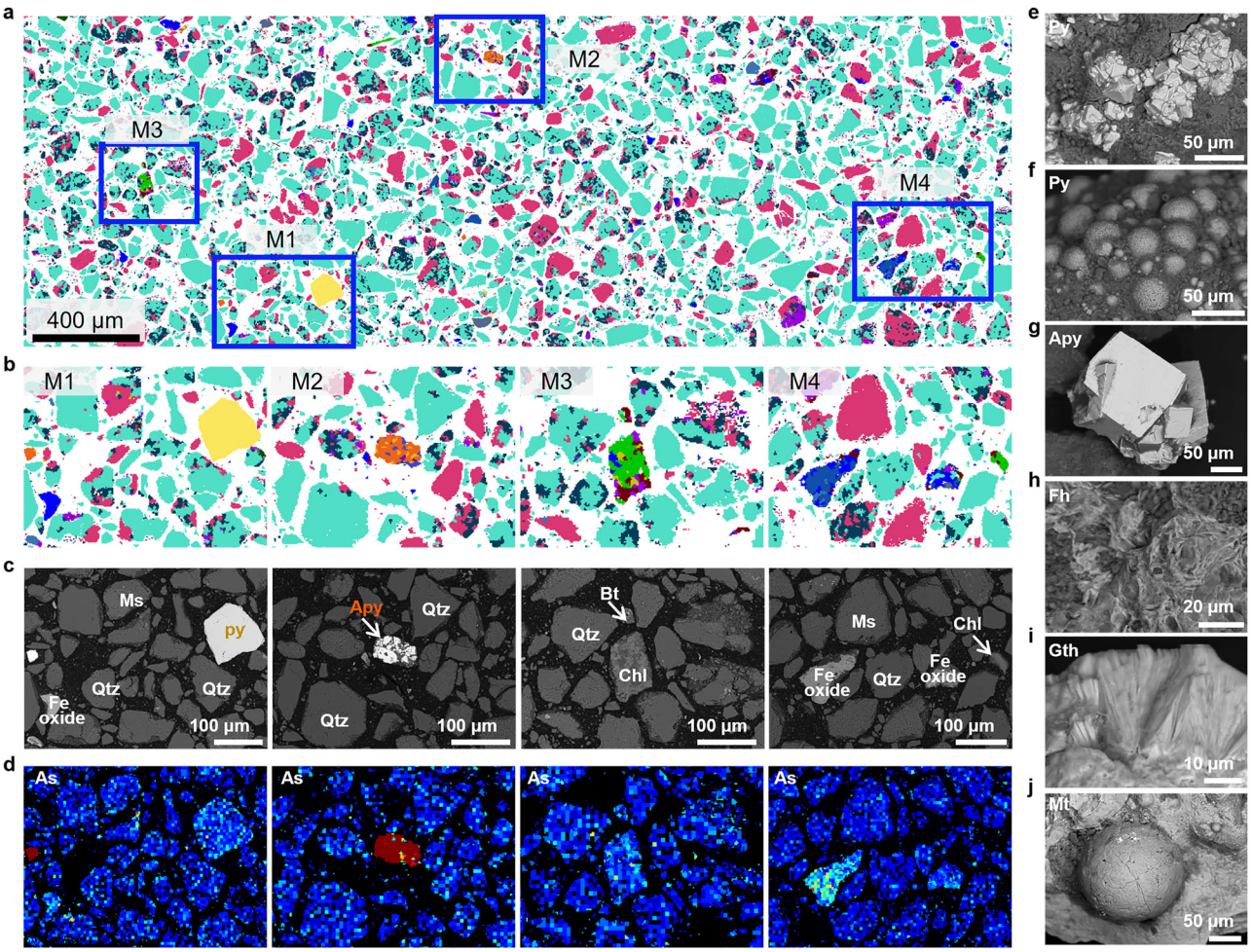

Fig. 3 | TIMA analysis of mineralogy and arsenic distribution in sample CG007-1. **a** Partial phase distribution map (1.2 × 3.6 mm). **b** Mineral phase distribution maps of M1-M4. **c** BSE images of regions M1-M4. **d** As element mapping of M1-M4. **e–j** BSE images of typical As-bearing minerals: Pyrite (cubic and framboidal), Arsenopyrite, Ferrihydrite, Goethite, Magnetite. Qtz quartz, Ms muscovite, Chl chlorite, Bt biotite.

environments supporting sulfide preservation and periodic redox fluctuations promoting Fe (hydr)oxide formation.

Scanning electron microscope (SEM) analysis revealed diverse morphologies of arsenic-bearing phases (Fig. 3e, f). Pyrite predominantly exhibited primary cubic crystals, indicating deep hydrothermal origins[34], while framboidal aggregates suggested secondary genesis in sedimentary environments with poorer weathering resistance and lower stability[35,36]. Arsenopyrite displayed columnar or prismatic crystals (Fig. 3g), implying mechanical migration during reclamation[37]. Fe (hydr)oxides showed varied morphologies (Fig. 3h-j), including needle-like goethite and flocculent ferrihydrite, reflecting different crystallinity and formation environments. These observations highlight the complex geochemical milieu for As retention and redistribution in reclaimed areas.

TIMA analysis combined with energy dispersive x-ray spectroscopy (EDS) showed marked variations in As content within As-bearing phases (Fig. 4). Arsenopyrite showed As:Fe molar ratios approaching 1:1 (As content 43.200-46.100 wt%), consistent with its theoretical composition and indicating minimal chemical alteration during reclamation. Arsenic-bearing pyrite exhibited more complex arsenic distribution, with As:S molar ratios reaching up to 0.09:1 (As content 8.430 wt%). EPMA further revealed microscopic heterogeneity in As distribution within pyrite, potentially resulting from multiple crystal growth stages and structural defects providing preferential sites for As enrichment[38].

Iron (hydr)oxides exhibited exceptionally high As:Fe molar ratios (up to 0.75:1, As content 33.96 wt%), suggesting potential co-precipitation of arsenate with ferrihydrite[39,40]. Heterogeneous As distribution within Fe oxides reflected the dynamic nature of As adsorption processes, influenced by local pH, redox potential and competing ions. The complex microstructure and varying crystallinity of iron oxides provided diverse binding sites and adsorption capacities for arsenic[30].

Silicates showed variations in As enrichment, with chlorite demonstrating the highest potential (arsenic content up to 9.64 wt%), followed by biotite (3.57 wt%) and illite (1.53 wt%). These differences likely as a result of the structural characteristics and chemical properties of these minerals. The interlayer hydroxyl groups in chlorite may provide additional binding sites for As, while the high Fe content in chlorite could enhance As retention through Fe-As complex formation[12,32]. The iron content in biotite also plays a crucial role in As retention, while the lower As content in illite may be due to its reduced specific surface area and fewer reactive sites[41].

Mineralogical observations closely aligned with BCR sequential extraction results, providing microscopic explanations for operationally defined arsenic speciation. Reclaimed areas exhibited a diverse assemblage of As-bearing phases, including sulfides, iron oxides and jarosite-like phases, explaining the higher content of oxidizable, reducible and acid-soluble As. This complex mineral assemblage reflects the unique reclamation history and dynamic redox environment. Vertical distribution patterns revealed incomplete sulfide oxidation in surface soils and a reducing environment in the subtidal zone, indicating a redox interface with potential microbially mediated geochemical cycling. Such dynamic equilibrium may lead to periodic transformation of As between different forms, increasing the complexity of environmental risks[28].

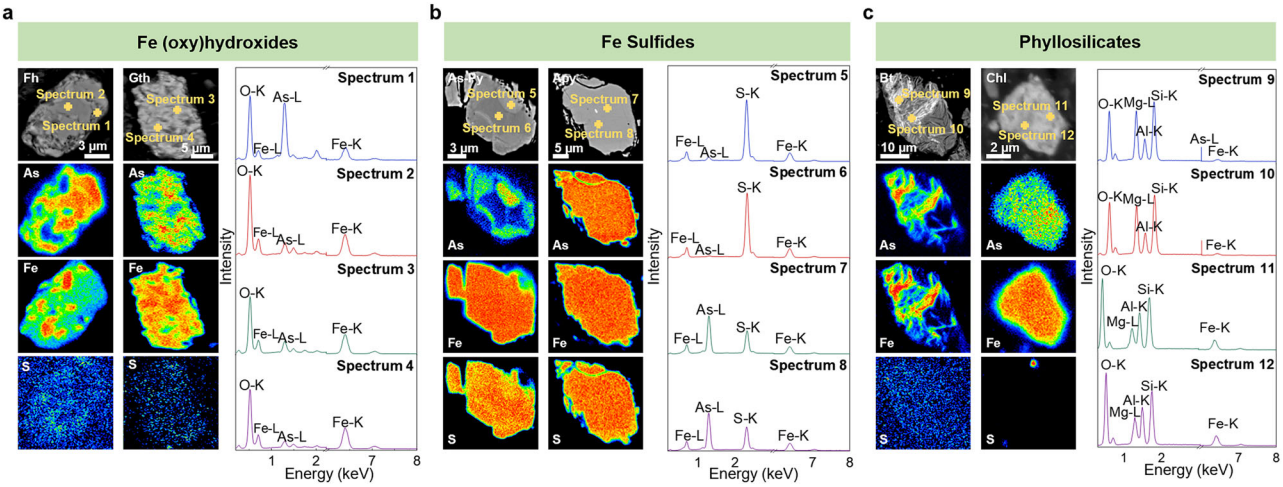

Fig. 4 | EPMA and EDS microanalysis of arsenic-bearing minerals in reclaimed soils. a Fe (hydr)oxides: ferrihydrite and goethite. **b** Fe sulfides: arsenian pyrite and arsenopyrite. **c** Phyllosilicates: biotite and chlorite. Each group: BSE images, As/Fe/S element maps and EDS spectra. Element maps: Brighter colors indicate higher concentrations. EDS spectra: Major characteristic peaks identified.

In contrast, hilly areas showed almost complete oxidation of primary sulfides due to long-term weathering, with As primarily in residual forms. However, an apparent discrepancy arose between high residual As content in BCR extraction and undetected As in many As-O species during TIMA analysis, likely due to TIMA's detection limits (<0.3 wt%). Therefore, high-sensitivity techniques (EPMA and LA-ICP-MS) were employed for in-depth analysis of low As concentration phases. This multi-technique approach provides comprehensive As distribution information across scales, enabling more accurate assessment of As behavior and risks in these complex soil systems.

Microanalysis of arsenic in low-content As-bearing phases

To characterize the distribution of trace As in As-O species undetectable by TIMA, we employed EPMA and LA-ICP-MS. These methods enabled elemental quantification of low-concentration As across different mineral phases. Figure 5 illustrates the partial analytical results, revealing the distribution characteristics of trace As in various As-O species.

EPMA analysis of low-As content goethite and biotite (Fig. 5a, b) revealed As presence below the EDS detection limit but detectable through the more sensitive WDS. Clear characteristic peaks in WDS spectra confirmed As in these minerals. Partial quantitative results (Supplementary Table S5) showed that among 12 selected Fe oxide locations, 5 points exhibited As content above the detection limit (0.089–0.787 wt%), with points 12–14 showing notably high As contents (0.787 wt%, 0.384 wt% and 0.474 wt%, respectively). In silicates (Supplementary Table S6), 4 out of 12 selected points contained detectable arsenic, with biotite (point 54) and kaolinite (point 108) showing relatively high contents (0.676 wt% and 0.372 wt%, respectively).

LA-ICP-MS analysis (Fig. 5c, d) further revealed trace As distribution characteristics in various mineral phases, demonstrating low-concentration As presence even in samples where EPMA failed to detect it. Time-resolved arsenic content curves exhibited variations with laser ablation depth, potentially reflecting microscopic heterogeneity of As in goethite and muscovite structures. Arsenic content in Fe (hydr)oxides ranged from 113.4 ppm to 6262.2 ppm, while silicates showed substantial variations, particularly the high concentration (7326.9 ppm) detected in biotite (Bio-1) (Supplementary Table S7). Arsenic content in kaolinite, illite and orthoclase ranged from 21.6 ppm to 386.1 ppm. Notably, a high As concentration (7120.7 ppm) was detected in the jarosite sample (Jar-1), indicating the role of these less easily oxidized secondary phases in As retention within sulfide oxidation environments.

These microscale analyses identify the high proportion of residual As observed in BCR extractions. The tight binding of As within mineral structures explains its predominance in difficult-to-extract residual forms. This strong fixation in iron oxides, certain silicates and secondary phases like jarosite suggests relatively low environmental risk associated with As in these phases. While localized high-concentration As areas may serve as potential release sources, the stable fixation of most arsenic within mineral structures indicates that any release process is likely to be slow and limited.

Discussion

Geogenic and anthropogenic influences on arsenic distribution and speciation

This study reveals differences in As enrichment and speciation between coastal reclaimed areas and hilly regions in urban soils, reflecting the combined influence of geological background and anthropogenic activities. Reclaimed soils display notably higher As content, locally reaching several hundred mg kg^{-1}, with spatial variability in As concentrations across the studied areas.

In reclaimed areas, As predominantly exists as As-S species (primary sulfides), originating from less weathered bedrock material used as fill. These materials likely derive from the deeper, unweathered portions of adjacent hilly regions, where As-rich rocks formed through regional tectonic activities and hydrothermal mineralization processes[11]. The reclamation process exposes these previously buried, sulfide-rich materials to surface conditions, accelerating their dissociation and redistribution. Arsenic mobilization from New Jersey coastal soils following storm-induced flooding has been documented[27], while tidal dynamics in Australian coastal areas have been shown to trigger arsenic release through iron-sulfur redox cycling[14]. These cases underscore the vulnerability of our study area to similar mobilization processes.

Conversely, surface soils in hilly areas show almost no sulfides, with As mainly associated with As-O species (Fe (hydr)oxides and silicates), reflecting extensive weathering of the exposed bedrock. This contrast highlights the difference in weathering intensity between the reclaimed materials and the long-exposed hilly surfaces. Recently formed reclaimed areas retain numerous sulfide minerals even in surface soils due to limited atmospheric exposure and oxidation. In contrast, hilly regions have undergone prolonged surficial weathering, resulting in the oxidation of primary As minerals and the predominance of As in secondary adsorbed or co-precipitated forms[32,42].

Our observations reveal complex geochemical controls on arsenic behavior in anthropogenically modified coastal soils. Traditional relationships between arsenic and soil properties (pH, organic matter) were weak, inadequately explaining arsenic distribution[30,40,41,43]. Moreover, mobile arsenic fractions showed no meaningful correlations with these parameters:

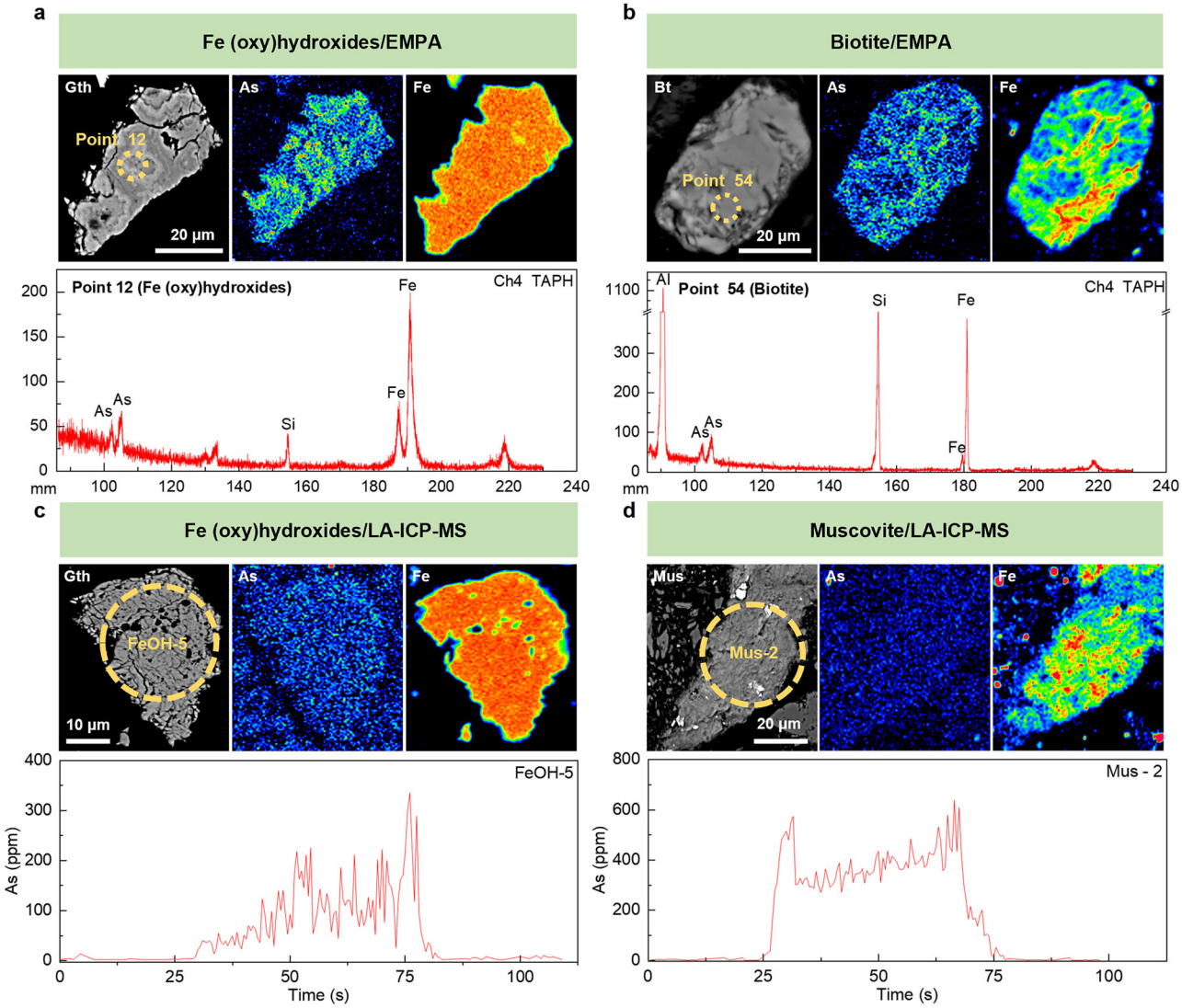

Fig. 5 | EPMA and LA-ICP-MS analysis of low-concentration arsenic in reclaimed soil minerals. a EPMA: Goethite (Point 12). **b** EPMA: Biotite (Point 54). **c** LA-ICP-MS: Goethite (FeOH-5). **d** LA-ICP-MS: Muscovite (Mus-2). EPMA panels. **a**, **b** BSE image, As/Fe maps, WDS spectrum (Ch4 TAPH crystal). LA-ICP-MS panels. **c**, **d** BSE image, As/Fe maps, time-resolved As concentration curve.

pH versus acid-soluble As (F1) and organic matter versus oxidizable As (F3) yielded negligible relationships. The dominance of mineral phase composition over bulk soil chemistry fundamentally alters arsenic behavior predictions.

Arsenic speciation in mineral phases and retention mechanisms

This research reveals distinct As occurrences in coastal reclaimed and hilly soils, with associated environmental risks. Sequential extraction analysis showed lower molar ratios of oxidizable As to S than theoretical values for arsenopyrite (FeAsS), attributed to incomplete oxidation of As-S species and re-adsorption during extraction[22]. BSE imaging demonstrated arsenopyrite with columnar or prismatic structures, where As occupies specific lattice positions, forming stable $Fe(As,S)_2$ structures resistant to short-term oxidation[37,44]. This explains the presence of substantial sulfides in both supratidal and subtidal zones of reclaimed areas.

Iron (hydr)oxides play a crucial role in As retention and migration. LA-ICP-MS analysis indicated the widespread presence of As in Fe (hydr) oxides, primarily as goethite and ferrihydrite. BSE imaging showed these minerals as discrete particles and coatings on silicates, considered secondary products of sulfides and Fe-bearing phases[45,46]. EDS and EPMA revealed high As/Fe molar ratios in ferrihydrite (up to 0.75) from reclaimed soils, exceeding typical adsorption scenarios. This aligns with findings by Fuller[47], who reported As(V)/Fe molar ratios up to 0.7 during As(V) co-precipitation with ferrihydrite, higher than adsorption scenarios (0.25). The structural basis for high arsenic loading was established by Waychunas[48], demonstrating bidentate binuclear complex formation at high surface coverage. This disparity may arise from reduced available surface area and active sites during ferrihydrite transformation to more stable crystalline phases[49–51].

Notably, BCR extraction revealed lower reducible As content than theoretically calculated from TIMA results, indicating persistent stable As forms in Fe (hydr)oxides after mild reducing treatments. Treatment of sample CG009-1 with $NH_2OH{\cdot}HCl$ showed partial reductive dissolution of ferrihydrite, with EPMA and EDS data revealing decreased As content in some particles post-dissolution (Supplementary Fig. S2). These observations align with studies by Tufano[52], noting inconsistencies between As release from ferrihydrite and As desorption during reduction-induced mineralogical transformation. It has been proposed that in Fe-rich samples, coprecipitation leads to arsenate forming bidentate binuclear complexes between primary ferrihydrite particles at diffusion-limited sites[22]. Consequently, a large proportion of As may be incorporated into the crystal structure of iron oxyhydroxides, potentially explaining the low As recovery observed in our BCR extraction. These structurally incorporated forms

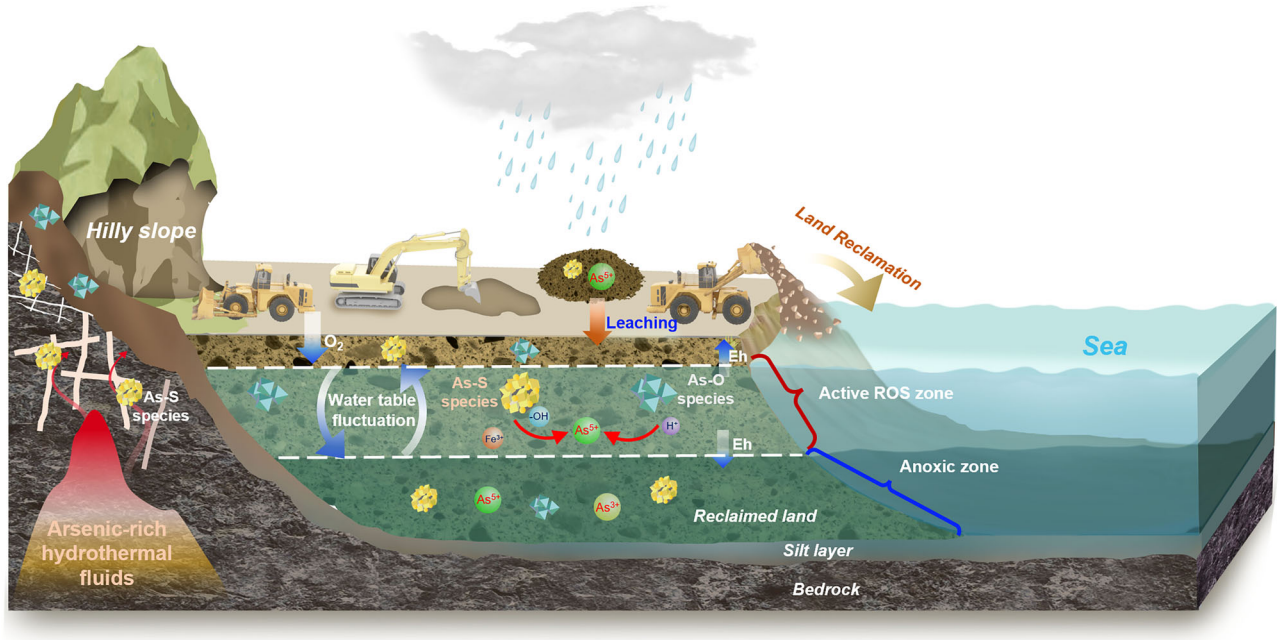

Fig. 6 | Conceptual figure illustrating the geochemical mobilization and environmental risk dynamics of geogenic arsenic in anthropogenically modified coastal Soils.

exhibit relative stability, constituting the primary residual As fraction. In moderately reducing environments, As typically resists reductive dissolution, remaining immobile and non-bioavailable. However, under strongly reducing conditions or over extended periods, even these stable forms may gradually mobilize[52].

Our investigation revealed abundant arsenic-bearing layered silicates in both reclaimed and hilly soils. Chlorite showed the highest arsenic adsorption affinity, followed by biotite, supporting findings by Manning[53] and Lin[54]. These phases constitute a large fraction of residual As, contrasting with Kreidie[55] who suggested minimal arsenic association with certain layered silicates. This discrepancy likely stems from our unique geological context and reclamation activities. To characterize the impact of oxidative conditions on silicates, we conducted TIMA analysis of reclaimed soil before and after the third step of the BCR sequential extraction procedure (H_2O_2 treatment). Results revealed localized oxidative alteration of chlorite and biotite structures without complete mineral decomposition. This process, likely due to partial oxidation of structural Fe^{2+} to Fe^{3+}, leads to surface degradation and release of bound arsenate species[32]. These findings highlight the potential for arsenic mobilization through oxidative dissolution of silicates. Additionally, As-bearing iron oxides often form associations with silicates as coatings or intergrowths, further complicating arsenic release mechanisms.

We also identified elevated concentrations of water-soluble and weak acid-extractable sulfur, indicating the presence of soluble sulfates. Water-soluble As concentrations in several samples exceeded regulatory thresholds (10 μg L^{-1}), signaling potential environmental risks. Concurrently, TIMA analysis revealed insoluble sulfates, predominantly jarosite, which EPMA and LA-ICP-MS confirmed as arsenic-bearing phases. Arsenic forms inner-sphere complexes on jarosite surfaces[56], but jarosite's high stability under acidic conditions contributes to the residual As fraction, potentially constraining arsenic bioavailability and environmental mobility[57].

Environmental behavior and risks of geogenic arsenic in coastal reclaimed soils

This work on coastal reclaimed soils expands the traditional perspective on heavy metal bioavailability. While exchangeable and acid-soluble fractions (i.e., those readily extractable by weak acids) are typically considered readily bioavailable, with reducible (bound to Fe/Mn oxides) and oxidizable (bound to organic matter and sulfides) forms showing relative stability[58,59], we found that previously stable As forms (As-S and As-O species) may transform into more mobile and bioavailable species in unique coastal environments, potentially increasing environmental and health risks (Supplementary Fig. S3). The higher proportions of non-residual arsenic fractions in reclaimed soils (mean 22.13%) compared to hilly soils (mean 6.93%) pose greater environmental and health risks due to enhanced bioavailability. Beyond direct soil exposure, arsenic enters aquatic food chains. Studies documented 0.42–3.44 mg kg^{-1} arsenic in PRD fish[60], and 57% of aquatic products exceeding standards[61], highlighting bioaccumulation risks from soil-water arsenic transfer.

The abundance of As-S species in coastal reclaimed soils constitutes a potential environmental risk, highlighting the crucial role of sulfide oxidation in As mobilization (Fig. 6). Future land development activities exposing these minerals to oxidizing environments could release As into the ecosystem, posing ecological and health risks. This risk is particularly pertinent given accelerating global coastal urbanization and the associated land reclamation practices, especially in regions rich in primary As-S species[7]. Environmental risks may vary globally due to factors such as geological background, reclamation material sources and climatic conditions. Sea-level rise and extreme weather trigger redox transitions mobilizing arsenic, while routine excavation and dewatering accelerate release, threatening water security and marine ecosystems across the region. Tropical and subtropical regions with hot, humid climates may face accelerated sulfide oxidation processes, increasing As release risk. Tidal fluctuations in coastal reclaimed areas further compound this risk, exacerbating As-S species oxidation, especially within the dynamic intertidal zone[28]. This cyclic wetting and drying process can lead to accelerated weathering of As-bearing minerals, enhancing As mobility.

As-O species, particularly As-bearing Fe (hydr)oxides like ferrihydrite and goethite, play a crucial role in As adsorption within coastal soils. While these phases can adsorb substantial amounts of As, they may release it through bioreduction under specific conditions such as sea-level rise or flooding[62]. In addition, we found limited reducible dissolved As content in iron oxides under natural conditions, suggesting their contribution to total As release may be less than that of oxidizable As from sulfide oxidation. However, in the context of global climate change, heavy metal pollution risks in reclaimed areas may be exacerbated. Sea-level rise could induce more frequent redox environment changes, promoting both reductive release of As from Fe hydroxides[27].

Seawater intrusion establishes reducing conditions where anaerobic bacteria convert As(V) to mobile As(III) through iron oxide dissolution[14]. Competitive ion exchange further enhances mobility[27], explaining As(V)/As(III) coexistence in anoxic zones (Fig. 6). Microbial methylation via arsM enzyme produces organic arsenic species (MMA, DMA), with enhanced activity in anaerobic coastal sediments[63]. Under reducing conditions, further transformation to volatile methylarsines may occur[64], affecting arsenic mobility and environmental fate. Photochemical processes may also contribute, as iron oxides generate reactive oxygen species under sunlight, driving arsenic redox cycling[65]. The elevated organic matter content in reclaimed soils potentially enhances these processes through ligand-to-metal charge transfer reactions[66]. While the extent of these photochemical transformations in our study area requires further investigation, they likely contribute to the complex arsenic cycling observed in reclaimed coastal environments.

Soil arsenic risk management framework for sustainable coastal urban development

Our findings reveal critical environmental risks from naturally occurring arsenic in coastal reclaimed areas, necessitating a comprehensive management framework that balances development needs with environmental protection.

Rigorous screening of fill materials before reclamation is paramount. Beyond meeting regulatory thresholds for total arsenic, source materials require mineralogical characterization to identify unstable As-S species and reactive As-O phases (e.g., ferrihydrite). Leaching tests under simulated marine conditions and sequential extraction must evaluate arsenic mobility potential, preventing future contamination scenarios.

Arsenic speciation data should guide zoning decisions. Areas dominated by unstable As-S minerals require restrictions on residential development and agriculture, while industrial uses with engineered controls (impermeable barriers, managed drainage) may be permissible. Buffer zones should separate high-risk areas from sensitive receptors including schools, water supplies and residential neighborhoods. Effective implementation requires engaging local stakeholders through transparent risk communication that incorporate local knowledge.

Long-term surveillance must track arsenic speciation changes, not merely total concentrations. Real-time monitoring at redox interfaces can detect transformation events triggering arsenic mobilization. Emergency protocols for extreme weather events should include alternative water supplies and accelerated sampling regimes. Community-based monitoring programs enhance coverage while building local capacity for risk management.

Current regulations designed for anthropogenic contamination poorly address geogenic arsenic lacking responsible parties. The heterogeneous distribution we documented resists uniform standards, while economic development pressures often override environmental concerns. Solutions include incorporating geogenic contamination into environmental impact assessments, developing flexible standards based on speciation rather than total concentration, and demonstrating economic benefits of proactive management through avoided remediation costs.

This research advances understanding of geogenic heavy metal behavior in anthropogenically modified environments, emphasizing the importance of integrating geochemical perspectives into urban planning. However, implementation faces challenges as regulations target anthropogenic rather than geogenic contamination, while heterogeneous arsenic distribution and economic pressures complicate enforcement. Future research should focus on developing in-situ speciation monitoring techniques, investigating microbial influences on arsenic transformation, and modeling arsenic behavior under climate change scenarios to further refine risk assessment and management approaches.

Methods

Soil sampling

Soil sampling was conducted in the PRD region of China, including three geomorphological units: reclaimed land, alluvial plain and hilly slopes. A total of 1029 soil samples from 312 locations were collected using profile excavation and core drilling techniques. Sampling depths varied by geomorphology: 0–20 m for land areas and 0–1.2 m for hilly slopes, reflecting the different soil development characteristics-deeper profiles in younger depositional environments with vertical heterogeneity versus shallower weathering zones in mature hill slope soils.

Sample site selection, based on land use records and field surveys, avoided known pollution sources to ensure samples represented naturally contaminated soils. This strategy minimized anthropogenic contamination, focusing on geogenic arsenic. Regional background arsenic values for the PRD average 11.2-11.9 mg kg^{-1} in natural soils (Shenzhen Soil Environmental Background Values, DB4403/T 68-2020), indicating that the elevated concentrations in our samples, particularly in reclaimed areas, represent geogenic enrichment. These measures ensured that collected samples primarily reflected arsenic derived from natural geological processes. Specific sampling locations are withheld due to land ownership restrictions.

Based on preliminary arsenic content analysis, 29 high-arsenic samples (As > 20 mg kg^{-1}) were selected from the initial 1029 for detailed geochemical and mineralogical study. This threshold exceeds local background values and soil environmental quality standard China (GB36600-2018) for arsenic. The selection criteria prioritized samples covering a wide range of arsenic concentrations while ensuring representation of diverse geographical locations. This subset comprised 14 samples from reclaimed land and 15 from hilly slopes, ensuring representation of both geomorphological units with their distinct environmental characteristics (Supplementary Table S8).

Sample pretreatment involved removing visible impurities and crushing the soil. Following collection, samples were stored at 4 °C and processed within 48 h. Air-drying proceeded at 20–25 °C for 5–7 days with daily mixing to ensure uniform moisture removal. Visible debris was removed using plastic tools, and samples were gently disaggregated with ceramic mortar and pestle to preserve mineral structures. Representative subsampling employed the coning and quartering method, repeated three times to minimize heterogeneity effects. The samples were then sieved through 2 mm (10 mesh) and 0.15 mm (100 mesh) stainless steel sieves to meet various analytical requirements. All equipment was cleaned with deionized water and dried between samples to prevent cross-contamination.

Bulk chemistry

Total arsenic content in soil samples was determined using microwave digestion coupled with hydride generation atomic fluorescence spectrometry (HG-AFS). The process began with microwave digestion of 0.5 g air-dried, sieved soil in a PTFE vessel, using 6 mL HCl ($\rho = 1.19$ g mL^{-1}) and 2 mL HNO_3 ($\rho = 1.42$ g mL^{-1}). This specific acid combination was selected in accordance with established protocols HJ 680–2013 to optimize arsenic extraction efficiency from various mineral phases. Following digestion, the solution acidity was adjusted, and a reducing agent solution (10 g thiourea and 10 g ascorbic acid in 100 mL ultrapure water) was added. Arsine generation was then performed using a freshly prepared potassium borohydride solution (1 g KBH_4 and 0.5 g KOH in 100 mL ultrapure water). The generated arsine produced atomic fluorescence when excited by an arsenic hollow cathode lamp. Finally, arsenic content was calculated based on the fluorescence intensity and a pre-established standard curve.

Total sulfur was determined by a turbidimetric method. A 0.1 g soil sample was mixed with magnesium nitrate solution, evaporated to dryness, and treated overnight in a 300 °C oven. After cooling, 25% nitric acid solution was added, followed by water bath digestion and filtration to a final volume of 50 mL. The filtrate was sequentially mixed with 50% acetic acid solution, 85% concentrated phosphoric acid and gum arabic solution. Barium chloride crystals were added to initiate the turbidimetric reaction. Sample absorbance was measured spectrophotometrically, and total sulfur content was calculated using a pre-established calibration curve. Total iron was quantified by acid digestion coupled with inductively coupled plasma mass spectrometry (ICP-MS) according to the United States Environmental

Protection Agency (EPA) Method 6020B. Soil samples were digested with a mixture of nitric acid, perchloric acid and hydrofluoric acid, followed by ICP-MS analysis to determine iron content.

Strict quality control and quality assurance measures were implemented to ensure analytical accuracy and reliability. Ten samples were randomly selected from the 29 soil samples and analyzed in triplicate to assess method precision. Blank tests were performed to check for potential contamination and interferences. Standard reference material GBW07405 (soil) was analyzed alongside samples to verify accuracy of total arsenic determination. The relative standard deviation (RSD) for all replicate sample measurements was maintained within 10%, ensuring robust and reproducible results.

Modified BCR sequential extraction for As, Fe and S speciation

This study employed a modified BCR sequential extraction method[20] to analyze the chemical speciation of arsenic, iron and sulfur in soil samples. The BCR approach was selected over alternative fractionation techniques due to its superior ability to differentiate arsenic associated with environmentally relevant phases in coastal soils, particularly iron oxides and sulfides. The procedure involved a three-step extraction process applied to 0.500 g of air-dried soil in a 50 mL polypropylene centrifuge tube. The acid-soluble fraction (F1) was extracted using 20 mL of 0.11 M CH_3COOH solution, followed by the reducible fraction (F2) with 20 mL of 0.5 M $NH_2OH{\cdot}HCl$ solution, and finally the oxidizable fraction (F3) with 8.8 M H_2O_2 and 1 M CH_3COONH_4 solution. Each extraction step was conducted under horizontal shaking for 16 h (180 ± 20 rpm) at room temperature, followed by centrifugation at 3000 g for 20 min. The resulting supernatant was filtered through a 0.45 μm membrane and stored at 0–4 °C for subsequent analysis. Between each extraction step, the residue was washed with 20 mL of ultrapure water, shaken for 15 min, and centrifuged at 3000 g for 20 min.

Arsenic content in the extracted supernatants was determined using atomic fluorescence spectrometry (AFS), while iron and sulfur were measured by inductively coupled plasma atomic emission spectroscopy (ICP-AES). Method accuracy was verified by comparing the sum of the extracted fractions to the total element content, with recoveries exceeding 90% for all samples. BCR-701 certified reference material (lake sediment) was used to validate the sequential extraction procedure, with measured values falling within certified ranges. For data reliability, seven of the 29 soil samples were randomly selected for triplicate analysis, maintaining RSD within 10% for most samples and not exceeding 15% for low-content samples near the detection limit.

Water-soluble arsenic was determined separately by mixing 1 g of soil with 20 mL ultrapure water, boiling, cooling to room temperature and shaking for 16 h at 200 rpm. The suspension was then centrifuged at 4500 g for 30 min, filtered through a 0.45 μm membrane, and the filtrate analyzed in triplicate by AFS.

Micro-scale characterization of As-bearing phases

Microanalysis was conducted on soil samples prepared via epoxy resin embedding, which involves encapsulating the soil particles in a solid matrix to enable grinding and polishing for microscopic examination. A mixture of 0.6 g soil and 2 g epoxy resin was ground and polished to adequately expose soil particles (Supplementary Note S1). To examine the original morphology of arsenic-bearing minerals, heavy mineral particles were separated from the soil and microscopically analyzed. Sample surfaces underwent cleaning with anhydrous ethanol, drying, and conductive treatment in a carbon coater (25 mA, 60 s, ~10 nm carbon film thickness) prior to analysis. A field emission scanning electron microscope (FE-SEM, TESCAN Mira-3) was employed to observe and analyze the original morphology of iron oxide and sulfide particles in the soil targets (Supplementary Note S2).

Comprehensive mineral phase analysis was conducted using a TIMA equipped with four energy dispersive spectrometers (EDAX Element 30). TIMA software v2.4.2 in release mode performed automatic identification analysis, simultaneously acquiring BSE images and EDS data. BSE images enabled particle identification and phase segmentation, with analysis points centered on the largest inscribed circle in each segmented area. Mineral identification utilized the TIMA software built-in database, comparing unknown minerals with standard spectral characteristics. Experimental parameters included an acceleration voltage of 25 kV, a current of 9.56 nA and a working distance of 15 mm. EDS signals were calibrated using a Mn standard, with X-ray counts set to 1000 per analysis point (Supplementary Table S9).

EPMA of arsenic-bearing minerals was performed using a JXA-iSP100 (control software v1.8.2) equipped with five spectrometers. EPMA mapping utilized an accelerating voltage of 15 kV, a current of 20 nA, a scanning step of 0.3–0.5 μm and a pixel scanning time of 50 ms. Quantitative analysis employed similar voltage and current, with a beam spot diameter of 3–10 μm. Peak position measurement times were 10 s for Fe and S and 60 s for As, with background measurements at half these durations. The ZAF method was applied for matrix correction. Major elements were analyzed using specific crystals: Fe (Kα, LiFL), S (Kα, PETJ) and As (Lα, TAP) (Supplementary Tables S10 and S11). Laser ablation-inductively coupled LA-ICP-MS analysis employed a 193 nm deep ultraviolet laser ablation system (Applied Spectra, Resolution SE) coupled with an Agilent 7900 ICP-MS. Instrument tuning followed Thompson[67], using a 100 μm spot size line scan on NIST 610 for P/A tuning. Sample surfaces were cleaned with methanol and pre-ablated to remove contamination. Analysis conditions included a 30 μm spot diameter, 5 Hz ablation frequency and 4.5 J cm^{-2} energy density. Data processing used the 3D Trace Element method in Iolite software v4[68]. Standard samples were analyzed every 2–5 sample points, with a typical analysis comprising 20 s of gas blank and 40 s of signal acquisition.

Reporting summary

Further information on research design is available in the Nature Portfolio Reporting Summary linked to this article.

Conclusion

This study comprehensively analyzes geogenic arsenic in coastal urban soils of China's PRD through integrated chemical and microscale techniques. Analysis of 1029 soil samples, with detailed characterization of 29 high-arsenic samples, reveals contrasting speciation patterns with critical environmental implications.

Reclaimed soils contain predominantly unstable As-S species (arsenopyrite, arsenian pyrite) resembling unweathered parent rock, while hilly soils show stable As-O associations with iron oxides and silicates from prolonged weathering. This fundamental difference creates divergent risk profiles: reclaimed areas face arsenic mobilization through land development, tidal dynamics and sea-level rise, whereas hilly soils exhibit minimal mobilization potential.

Our multi-technique approach-combining BCR extraction with TIMA, EPMA and LA-ICP-MS-enabled identification of diverse As-bearing phases across concentration ranges, revealing previously unrecognized As retention mechanisms in complex soil matrices. This methodology advances beyond traditional single-technique limitations.

Based on these mechanistic insights, we propose an integrated management framework incorporating risk-based land-use planning, source material screening and adaptive monitoring systems. The framework addresses the unique challenges of geogenic contamination in anthropogenically modified coastal environments.

This research underscores that sustainable coastal urbanization requires understanding natural contaminant behavior under changing environmental conditions. Climate change amplifies arsenic mobilization through sea-level rise, extreme weather events and accelerated geochemical processes. The unstable As-S species in reclaimed soils are particularly vulnerable to these impacts, necessitating integration of climate adaptation with geochemical risk management. As coastal development accelerates globally, our findings provide essential guidance for managing geogenic arsenic risks while supporting urban growth in vulnerable coastal regions.

Data availability

Data for this manuscript are available at Zenodo with the following link: https://doi.org/10.5281/zenodo.16250152.

Received: 5 January 2025; Accepted: 25 July 2025;
Published online: 06 August 2025

References

1. Martín-Antón, M., Negro, V., del Campo, J. M., López-Gutiérrez, J. S. & Esteban, M. D. Review of coastal land reclamation situation in the world. *J. Coast. Res.* **667**, 671 (2016).
2. Chee, S. Y., Othman, A. G., Sim, Y. K., Mat Adam, A. N. & Firth, L. B. Land reclamation and artificial islands: walking the tightrope between development and conservation. *Glob. Ecol. Conserv.* **12**, 80–95 (2017).
3. Sengupta, D., Chen, R. & Meadows, M. E. Building beyond land: an overview of coastal land reclamation in 16 global megacities. *Appl. Geogr.* **90**, 229–238 (2018).
4. Wang, W., Liu, H., Li, Y. & Su, J. Development and management of land reclamation in China. *Ocean Coast. Manag.* **102**, 415–425 (2014).
5. Hu, Y. et al. Assessing heavy metal pollution in the surface soils of a region that had undergone three decades of intense industrialization and urbanization. *Environ. Sci. Pollut. Res.* **20**, 6150–6159 (2013).
6. Zhang, G. et al. Heavy metal fractions and ecological risk assessment in sediments from urban, rural and reclamation-affected rivers of the Pearl River Estuary, China. *Chemosphere* **184**, 278–288 (2017).
7. Itabashi, T. et al. Speciation and fractionation of soil arsenic from natural and anthropogenic sources: chemical extraction, scanning electron microscopy, and micro-XRF/XAFS investigation. *Environ. Sci. Technol.* **53**, 14186–14193 (2019).
8. Chen, M. et al. Source identification and exposure risk management for soil arsenic in urban reclamation areas with high background levels: a case study in a coastal reclamation site from the Pearl River Delta, China. *J. Hazard. Mater.* **465**, 133294 (2024).
9. Li, H. et al. Geochemistry and geochronology of the Banxi Sb deposit: implications for fluid origin and the evolution of Sb mineralization in central-western hunan, South China. *Gondwana Res.* **55**, 112–134 (2018).
10. Mei, J. et al. Effects of human enclosure and farming activities on heavy metals in sediments/soils of the coastal reclamation areas in the Yangtze estuary. *J. Soils Sediment.* **22**, 2435–2447 (2022).
11. Smedley, P. L. & Kinniburgh, D. G. A review of the source, behaviour and distribution of arsenic in natural waters. *Appl. Geochem.* **17**, 517–568 (2002).
12. Campbell, K. M. & Nordstrom, D. K. Arsenic speciation and sorption in natural environments. *Rev. Mineral. Geochem.* **79**, 185–216 (2014).
13. Sharma, V. K. & Sohn, M. Aquatic arsenic: toxicity, speciation, transformations, and remediation. *Environ. Int.* **35**, 743–759 (2009).
14. Burton, E. dwardD. et al. Arsenic mobility during flooding of contaminated soil: the effect of microbial sulfate reduction. *Environ. Sci. Technol.* **48**, 13660–13667 (2014).
15. Foster, A. L., Brown, G. E., Tingle, T. N. & Parks, G. A. Quantitative arsenic speciation in mine tailings using X-ray absorption spectroscopy. *Am. Mineralog* **83**, 553–568 (1998).
16. Nordstrom, D. K. Worldwide occurrences of arsenic in ground water. *Science* **296**, 2143–2145 (2002).
17. Nickson, R. et al. Arsenic poisoning of Bangladesh groundwater. *Nature* **395**, 338–338 (1998).
18. Tessier, A., Campbell, P. G. C. & Bisson, M. Sequential extraction procedure for the speciation of particulate trace metals. *Anal. Chem.* **51**, 844–851 (1979).
19. Tack, F. M. G. & Verloo, M. G. Chemical speciation and fractionation in soil and sediment heavy metal analysis: a review. *Int. J. Environ. Anal. Chem.* **59**, 225–238 (1995).
20. Rauret, G. et al. Improvement of the BCR three step sequential extraction procedure prior to the certification of new sediment and soil reference materials. *J. Environ. Monit.* **1**, 57–61 (1999).
21. Bacon, J. R. & Davidson, C. M. Is there a future for sequential chemical extraction?. *Analyst* **133**, 25–46 (2008).
22. Van Herreweghe, S., Swennen, R., Vandecasteele, C. & Cappuyns, V. Solid phase speciation of arsenic by sequential extraction in standard reference materials and industrially contaminated soil samples. *Environ. Pollut.* **122**, 323–342 (2003).
23. Barnes, S. J. et al. Primary cumulus platinum minerals in the Monts de Cristal Complex, Gabon: magmatic microenvironments inferred from high-definition X-ray fluorescence microscopy. *Contrib. Miner. Pet.* **171**, 23 (2016).
24. Lintern, M. J., Hough, R. M., Ryan, C. G., Watling, J. & Verrall, M. Ionic gold in calcrete revealed by LA-ICP-MS, SXRF and XANES. *Geochim. Cosmochim. Acta* **73**, 1666–1683 (2009).
25. Nriagu, J. O. et al. Arsenic in soil and groundwater: an overview. *Trace Met. Other Contam. Environ.* **9**, 3–60 (2007).
26. Ran, H. et al. Pollution characteristics and environmental availability of toxic elements in soil from an abandoned arsenic-containing mine. *Chemosphere* https://doi.org/10.1016/j.chemosphere.2022.135189 (2022).
27. LeMonte, J. J. et al. Sea level rise induced arsenic release from historically contaminated coastal soils. *Environ. Sci. Technol.* **51**, 5913–5922 (2017).
28. Zhao, G. et al. Redox oscillations activate thermodynamically stable iron minerals for enhanced reactive oxygen species production. *Environ. Sci. Technol.* **57**, 8628–8637 (2023).
29. Wei, Y. et al. A critical review of groundwater table fluctuation: formation, effects on multifields, and contaminant behaviors in a soil and aquifer system. *Environ. Sci. Technol*. **58**, 2185–2203 (2024).
30. Dixit, S. & Hering, J. G. Comparison of arsenic(V) and arsenic(III) sorption onto iron oxide minerals: implications for arsenic mobility. *Environ. Sci. Technol.* **37**, 4182–4189 (2003).
31. Drahota, P. & Filippi, M. Secondary arsenic minerals in the environment: a review. *Environ. Int.* **35**, 1243–1255 (2009).
32. Masuda, H. et al. Sequential chemical extraction of arsenic and related elements from the Holocene sediments of Sonargaon, Bangladesh, in relation to formation of arsenic-contaminated groundwater. *Geochem. J.* **47**, 651–661 (2013).
33. Cui, J. et al. Speciation, mobilization, and bioaccessibility of arsenic in geogenic soil profile from Hong Kong. *Environ. Pollut.* **232**, 375–384 (2018).
34. Gu, X., Heaney, P. J., Reis, F. D. A. A. & Brantley, S. L. Deep abiotic weathering of pyrite. *Science* **370**, eabb8092 (2020).
35. Savage, K. S., Tingle, T. N., O'Day, P. A., Waychunas, G. A. & Bird, D. K. Arsenic speciation in pyrite and secondary weathering phases, Mother Lode Gold District, Tuolumne County, California. *Appl. Geochem.* **15**, 1219–1244 (2000).
36. Wilkin, R. T., Barnes, H. L. & Brantley, S. L. The size distribution of framboidal pyrite in modern sediments: an indicator of redox conditions. *Geochim. Cosmochim. Acta* **60**, 3897–3912 (1996).
37. Corkhill, C. L., Corkhill, C. L., Vaughan, D. J. & Vaughan, D. J. Arsenopyrite oxidation—a review. *Appl. Geochem.* https://doi.org/10.1016/j.apgeochem.2009.09.008 (2009).
38. Deditius, A. P. et al. A proposed new type of arsenian pyrite: Composition, nanostructure and geological significance. *Geochim Cosmochim. Ac* **72**, 2919–2933 (2008).
39. Suda, A. & Makino, T. Functional effects of manganese and iron oxides on the dynamics of trace elements in soils with a special focus on arsenic and cadmium: a review. *Geoderma* **270**, 68–75 (2016).
40. Wenzel, W. W. Arsenic. in *Heavy Metals in Soils* Vol. 22 (ed Alloway, B. J.) (Springer Netherlands, 2013).

41. Chakraborty, S., Wolthers, M., Chatterjee, D. & Charlet, L. Adsorption of arsenite and arsenate onto muscovite and biotite mica. *J. Colloid Interface Sci.* **309**, 392–401 (2007).
42. Brammer, H. & Ravenscroft, P. Arsenic in groundwater: a threat to sustainable agriculture in south and south-east Asia. *Environ. Int.* **35**, 647–654 (2009).
43. Goldberg, S. Competitive adsorption of arsenate and arsenite on oxides and clay minerals. *Soil Sci. Soc. Am. J.* **66**, 413–421 (2002).
44. Hongxin, Q. et al. Study on the influence of active oxygen on the natural oxidation of arsenopyrite under different temperature conditions. *J. Hazard. Mater.* **478**, 135420 (2024).
45. Drahota, P. et al. Mineralogical and geochemical controls of arsenic speciation and mobility under different redox conditions in soil, sediment and water at the Mokrsko-West gold deposit, Czech Republic. *Sci. Total Environ.* **407**, 3372–3384 (2009).
46. Fendorf, S., Nico, P. S., Kocar, B. D., Masue, Y. & Tufano, K. J. Arsenic chemistry in soils and sediments. *Synchrotron-Based Tech. Soils Sediment.* **34**, 357–378 (2010).
47. Fuller, C. C., Davis, J. A. & Waychunas, G. A. Surface chemistry of ferrihydrite: part 2. Kinetics of arsenate adsorption and coprecipitation. *Geochim. Cosmochim. Acta* **57**, 2271–2282 (1993).
48. Waychunas, G. A., Davis, J. A. & Fuller, C. C. Geometry of sorbed arsenate on ferrihydrite and crystalline FeOOH: Re-evaluation of EXAFS results and topological factors in predicting sorbate geometry, and evidence for monodentate complexes. *Geochim. Cosmochim. Acta* **59**, 3655–3661 (1995).
49. Appelo, C. A. J., Van Der Weiden, M. J. J., Tournassat, C. & Charlet, L. Surface complexation of ferrous iron and carbonate on ferrihydrite and the mobilization of arsenic. *Environ. Sci. Technol.* **36**, 3096–3103 (2002).
50. Hansel, C. M. et al. Secondary mineralization pathways induced by dissimilatory iron reduction of ferrihydrite under advective flow. *Geochim. Cosmochim. Acta* **67**, 2977–2992 (2003).
51. Hong, J., Liu, L., Ning, Z., Liu, C. & Qiu, G. Synergistic oxidation of dissolved As(III) and arsenopyrite in the presence of oxygen: Formation and function of reactive oxygen species. *Water Res.* **202**, 117416 (2021).
52. Tufano, K. J. & Fendorf, S. Confounding impacts of iron reduction on arsenic retention. *Environ. Sci. Technol.* **42**, 4777–4783 (2008).
53. Manning, B. A. & Goldberg, S. Adsorption and stability of arsenic(III) at the clay mineral−water interface. *Environ. Sci. Technol.* **31**, 2005–2011 (1997).
54. Lin, Z. & Puls, R. W. Adsorption, desorption and oxidation of arsenic affected by clay minerals and aging process. *Environ. Geol.* **39**, 753–759 (2000).
55. Kreidie, N. et al. An integrated geochemical and mineralogical approach for the evaluation of arsenic mobility in mining soils. *J. Soils Sediment.* **11**, 37–52 (2011).
56. Asta, M. P., Cama, J., Martínez, M. & Giménez, J. Arsenic removal by goethite and jarosite in acidic conditions and its environmental implications. *J. Hazard. Mater.* **171**, 965–972 (2009).
57. Bigham, J. M. & Nordstrom, D. K. Iron and aluminum hydroxysulfates from acid sulfate waters. *Rev. Mineral. Geochem.* **40**, 351–403 (2000).
58. Filgueiras, A. V., Lavilla, I. & Bendicho, C. Chemical sequential extraction for metal partitioning in environmental solid samples. *J. Environ. Monit.* **4**, 823–857 (2002).
59. Li, J. et al. Investigations of water-extractability of As in excavated urban soils using sequential leaching tests: effect of testing parameters. *J. Environ. Manage*. https://doi.org/10.1016/j.jenvman.2018.03.105 (2018).
60. Cheung, K. C., Leung, H. M. & Wong, M. H. Metal concentrations of common freshwater and marine fish from the Pearl River Delta, south China. *Arch. Environ. Contam Toxicol.* **54**, 705–715 (2008).
61. Rao, M. et al. Trace elements in aquatic products from Shenzhen, China and their implications for human exposure. *Sci. Total Environ.* **885**, 163726 (2023).
62. Tabelin, C. B. et al. Arsenic, selenium, boron, lead, cadmium, copper, and zinc in naturally contaminated rocks: a review of their sources, modes of enrichment, mechanisms of release, and mitigation strategies. *Sci. Total Environ.* https://doi.org/10.1016/j.scitotenv.2018.07.103. (2018).
63. Zhao, F.-J. et al. Arsenic methylation in soils and its relationship with microbial *arsM* abundance and diversity, and As speciation in rice. *Environ. Sci. Technol.* **47**, 7147–7154 (2013).
64. Mestrot, A. et al. Field Fluxes and Speciation of Arsines Emanating from Soils. *Environ. Sci. Technol.* **45**, 1798–1804 (2011).
65. Shu, Z. et al. Sunlight-induced interfacial electron transfer of ferrihydrite under oxic conditions: mineral transformation and redox active species production. *Environ. Sci. Technol.* **56**, 14188–14197 (2022).
66. Wang, C. et al. Sunlight-driven transformation of ferrihydrite via ligand-to-metal charge transfer: the critical factors and arsenic repartitioning. *Environ. Sci. Technol*. https://doi.org/10.1021/acs.est.4c11046 (2025).
67. Naujokas, M. F. et al. The broad scope of health effects from chronic arsenic exposure: update on a worldwide public health problem. *Environ. Health Perspect.* **121**, 295–302 (2013).
68. Paul, B. et al. Time resolved trace element calibration strategies for LA-ICP-MS. *J. Anal. Spectrom.* **38**, 1995–2006 (2023).

Acknowledgements

This work was supported by the National Key Research and Development Program of China (Grant No. 2023YFC3706005 and 2018YFC1801100). We are grateful to the local environmental protection bureaus for their assistance during field investigations.

Author contributions

M. C., T. L., and L. W. conceptualized and designed the research. Y. L. and Z. S. designed and conducted the field sampling campaign. M. C., Y. L. and Y. Z. performed chemical extraction experiments and data analysis. W. J. designed and conducted microscale characterization experiments. M. C. and T. L. wrote the original draft. T. L. and L. W. supervised the project and provided critical guidance throughout the study. All authors contributed to manuscript revision and approved the final version.

Competing interests

The authors declare no competing interests.

Additional information

Supplementary information The online version contains supplementary material available at https://doi.org/10.1038/s43247-025-02634-1.

Correspondence and requests for materials should be addressed to Lei Wang or Tao Long.

Peer review information *Communications Earth and Environment* thanks Albert Kobina Mensah and the other, anonymous, reviewer(s) for their contribution to the peer review of this work. Primary Handling Editors: Somaparna Ghosh.